
CHAPTER 4

Biological Applications of Electrostatic Calculations and Brownian Dynamics Simulations

Jeffrey D. Madura*, Malcolm E. Davis†, Michael K.
Gilson‡, Rebecca C. Wade§, Brock A. Luty‡,
and J. Andrew McCammon‡

**University of South Alabama, Department of Chemistry,
Mobile, Alabama 36688 †Bristol Myers-Squibb Pharmaceutical
Research Institute, P.O. Box 4000, Princeton, New Jersey
08543 ‡University of Houston, Department of Chemistry,
Houston, Texas 77204 and §European Molecular Biology
Laboratory, Meyerhofstrasse 1, 6900 Heidelberg, Germany*

INTRODUCTION

Large biological molecules, such as superoxide dismutase (SOD), triose phosphate isomerase (TIM), acetylcholinesterase, rhinovirus, bacteriorhodopsin, antibodies, RNA, and DNA, have become accessible to theoretical study recently as a result of the availability of modern computers and sophisticated theories.^{1,2} Two rapidly emerging areas of interest are the computation of electrostatic interactions using continuum models³⁻⁵ and the simulation of diffusional motion in biopolymers and the diffusional encounters between lig-

ands and their receptors based on Brownian dynamics.⁶ With continuum electrostatic methods, one is able to calculate accurate electrostatic energies and forces for ionizable groups in small molecules and biopolymers, determine accurate electrostatic free energies of solvation, and compute relative electrostatic free energies of binding. Brownian dynamics, on the other hand, extends the time frame for studying motions in enzymes, e.g., loop movements and hinge-bending motion. One can now begin to investigate motions that are in the nanosecond-to-microsecond range. Brownian dynamics coupled with continuum electrostatics can be used to understand the effects of electrostatics on the rate at which a substrate approaches a target enzyme. This has proven to be a valuable approach in the design of mutants of superoxide dismutase, which have increased catalytic activities.⁷

The goal of this chapter is to provide the reader with a resource covering a variety of computational methods. In keeping with this objective, we give an overview of electrostatics and Brownian dynamics and also a minitutorial for the University of Houston Brownian Dynamics (UHBD) program.⁸ Although we do not attempt to provide a comprehensive review, the references cited should provide a good entryway into the literature. Keep in mind that the electrostatic principles and examples presented here are applicable to other programs such as DelPhi^{8,9} and MEAD,⁸ as well. In this chapter, we consider first the application of continuum electrostatics to the calculation of energies and forces, then electrostatics coupled with Brownian dynamics simulations. Model systems of small molecules and proteins will be used to demonstrate the application and utility of these methods. Each section begins with a short review of the theory, followed by appropriate applications, and, in certain cases, sample calculations using the UHBD program.

BROWNIAN DYNAMICS SIMULATIONS

Theory

Brownian dynamics is a method to simulate the diffusive behavior of a system of N interacting particles. Some degrees of freedom of the system are treated explicitly, while others are represented by their stochastic influence on the former ones. When the solvent frictional effects on the explicit solute particles are large enough to damp inertial displacements of the solute, one has Brownian dynamics; otherwise a more general stochastic dynamics model can be used to describe the solute motion. Various algorithms have been developed to perform Brownian or stochastic dynamics simulations.⁵⁸ The stochastic dynamics methods are generally based on the traditional deterministic molecular dynamics approach as opposed to the “Monte Carlo” approach used by Ermak and McCammon for Brownian dynamics. Only the Ermak–McCammon approach is discussed here because it has been widely applied to the study of diffusion-controlled rate processes, which is a major theme of this chapter. The Ermak–McCammon method⁵⁹ for computing Brownian dynamic trajectories is most easily introduced by considering the following one-dimensional example. A particle is placed at an initial position x_0 . From the analytical form of the probability distribution function for particle displacements, a new position at Δt is randomly chosen. Therefore the first step of a diffusional trajectory is

$$x = x_0 + R \quad [36]$$

where R is a random number with the statistical properties $\langle R \rangle = 0$ and $\langle R^2 \rangle = 2D\Delta t$. The trajectory is extended to $t = 2\Delta t$, $t = 3\Delta t$, etc., by sampling

distributions that are centered at the position found during the previous time step. This procedure yields one representative diffusional trajectory. By computing a large number of such trajectories with different sets of random numbers, one generates a description of how an ensemble of diffusing molecules behaves.

The generalization of Eq. [36] for the case of a particle diffusing in three dimensions relative to a second particle and subject to an arbitrary force is

$$\mathbf{r} = \mathbf{r}_0 + (k_B T)^{-1} D \mathbf{F}(\mathbf{r}_0) \Delta t + \mathbf{R} \quad [37]$$

where \mathbf{r}_0 is the position before a step is taken, k_B is Boltzmann's constant, T is the temperature, D is the relative diffusion constant, $\mathbf{F}(\mathbf{r}_0)$ is the force between the two particles at \mathbf{r}_0 , Δt is the time step, and \mathbf{R} is a random vector with statistical properties $\langle \mathbf{R} \rangle = 0$ and $\langle R_i R_j \rangle = 2D \delta_{ij} \Delta t$. Equation [37] can be further generalized to treat structured entities, hydrodynamic interactions, etc.⁵⁹⁻⁶¹ The time step Δt in any region should be so small that the force on the particle changes by only about 10% or less during any step. Longer time steps can be achieved at some additional computing cost by using a second-order algorithm⁶² instead of the first-order algorithm in Eq. [37].

The Brownian dynamics method described above can be used to generate diffusional trajectories of a substrate in the field of an enzyme target.^{7,8,60,61,64-71} To calculate a rate constant, the probability β of a substrate diffusing from some given initial separation and reacting with the fixed enzyme is calculated. It is this probability that is used to calculate the diffusion-controlled rate constant. (If the substrate is large, it may be necessary to allow for rotational diffusion of the target enzyme.^{67,72} Also, the assumption of a translationally fixed target is strictly valid only for dilute systems.⁷³ The space around the enzyme is divided by a spherical surface of radius b into an outer region ($r > b$) and an inner region ($r < b$) (see Figure 3). Trajectories of the substrate are initiated on the surface of this sphere. The value of b is usually chosen to be sufficiently large that the interparticle forces between the pair are approximately centrosymmetric for $r > b$. Thus, any effect of charge asymmetry of the species has a negligible effect on translational diffusion at distances $r > b$. This condition, which allows for the simplest simulation procedure, can be relaxed to increase computational efficiency. An outer spherical surface of radius q is defined as a truncation surface, at which any trajectories that wander too far from the target particle are terminated. A correction must be applied to the combination probability to allow for the possibility that untruncated trajectories could recross the q surface and react with the target particle. As shown by Zhou, q should be chosen to be sufficiently large that the inward reactive flux at this distance is centrosymmetric in the reaction being modeled.⁷⁴

The value of q is not known a priori but is typically several times larger than the value of b . This implies that a vast majority of the space in which the diffusion is simulated is between the b and the q surfaces, where the potential is

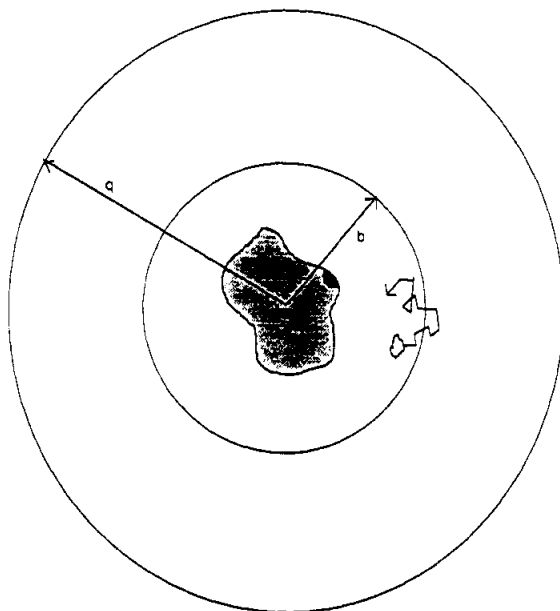


Figure 3 General schematic picture for computation of bimolecular rate constants by Brownian dynamics simulation. The “sphere” at radius b represents the division of space into an anisotropic inner region and an isotropic outer region, while the “sphere” at radius q is for outer trajectory truncation. Electrostatic potential energy contours would be irregular inside the sphere of radius b and centrosymmetric outside.

spherically symmetric. Recently, we proposed a method that takes advantage of the one-dimensional nature of the potential in this region.⁷⁵ Briefly, if the particle diffuses outside the b surface, a pretabulated solution to the diffusion equation is used to determine whether the particle would escape to infinity or return to some location on the b surface. This method can be quite efficient, typically cutting the computational time by one-half or more.

Calculation of the reaction probability for a pointlike substrate without electrostatics is accomplished using the following algorithm.

1. Define the b and q surfaces with respect to the center of the target. Typical values for the b surface are on the order of 70–100 Å while for the q surface they are on the order of 300–500 Å.
2. Randomly place the substrate on the b surface, (r_0).
3. Calculate the substrate’s new position (r) using Eq. [37].
4. Test to determine if the particle (a) reacted, (b) went beyond the q surface, or (c) was unreactive but not beyond the q surface.
 - (a) (reacted) Count the trajectory as successful and go to step 2.
 - (b) (beyond the q surface) Truncate the trajectory and count the trajectory as unsuccessful and go to step 2.
 - (c) (unreactive) Set r of the preceding step to r_0 and go to step 3.
 Repeat steps 3 and 4 until several hundreds or thousands of trajectories have been generated.
5. When a sufficient number of trajectories have been run, calculate β , which is the number of successful trajectories divided by the total number of trajectories initiated.

With the probability of reaction, the rate constant is given by

$$k = k_D(b)\beta[1 - (1 - \beta)\Omega]^{-1} \quad [38]$$

Here, $k_D(b)$ is the steady state rate at which mobile reactants with $r > b$ would first strike the spherical surface at $r = b$, and β is the computed reaction probability. With the assumptions that the interparticle potential U is centrosymmetric and the hydrodynamic interaction is negligible for $r > b$, $k_D(b)$ is given by

$$k_D(b) = 4\pi \left[\int_b^\infty \left(\frac{e^{U(r)/k_B T}}{r^2 D} \right) dr \right]^{-1} \quad [39]$$

The quantity Ω is given by

$$\Omega = \frac{k_D(b)}{k_D(q)} \quad [40]$$

Where Ω is the probability that a particle at $r = q$ will eventually return to $r = b$.

The same procedure is used when electrostatics is incorporated into the calculation except that the electrostatic grid is computed before step 1. The grid is determined by first placing the target on a grid, defining the high and low dielectric regions, assigning charges, then solving the PB equation using the finite difference approaches discussed earlier.

The most straightforward way of determining the reaction probability β is to simply carry out a large number of trajectories (say N) and equate β to the fraction of trajectories that reach the active site (free diffusion approach). Implicit in Eq. [38] and the statistical properties of the random displacement vector \mathbf{R} is the assumption that diffusional displacements in Δt are small, on the average, compared to distances from absorbing and/or reflecting boundaries. This condition can be satisfied by choosing Δt small enough. A more general approach to this problem is the probability distribution method developed by Lamm and Schulten⁷⁶ and Northrup et al.⁷⁷. In this method, account of boundaries is taken in generating \mathbf{R} , which makes longer time steps permissible. Northrup et al. showed that survival probabilities w_i can then be computed for each trajectory i and that

$$\beta = \frac{\sum_{i=1}^N w_i}{N} \quad [41]$$

The survival probability is computed from

$$w_i = \prod_k w_{ik} \quad [42]$$

where w_{ik} is the survival probability of the k th dynamics step of the i th trajectory. The w_{ik} , in turn, are given by

$$w_{ik} = \frac{p_{\text{react}}}{p_{\text{reflect}}} \quad [43]$$

Here, p_{react} is the probability of the substrate initially at \mathbf{r}_0 ending up at \mathbf{r} (Eq. [37]), determined from the short-time solution of the diffusion equation with the active site taken to be perfectly absorbing, i.e., every collision results in a reaction, or partially absorbing. On the other hand, p_{reflect} is the corresponding probability when the active site is treated as a reflective boundary. Analytic expressions for these probabilities can be found elsewhere.^{76–78} In addition to allowing larger time steps near boundaries, the probability distribution method has the useful advantage that multiple rate constants (for different reactivity criteria) can be determined in a single simulation. Northrup and co-workers have applied this method, with perfectly absorbing active sites, to carbonic anhydrase⁷⁹ and heme proteins.⁸⁰ Recently the partially absorbing case has been studied for simple model systems.⁷⁸

Before closing the theory section, it should be mentioned that simulations also can be used to study “gated” reactions, in which the reactivity criteria vary in time, perhaps reflecting internal motions in the target. The dynamics of the gate can be described most simply by the rate constants k_c and k_o , rate constants for closing and opening the gate (i.e., turning the target reactivity off or on). Restricting the discussion to stochastic gating, suppose the gate was open/closed during the preceding dynamics step and that a dynamics step of duration Δt is now to be taken. The probability p_g that the gate remains open/closed is

$$p_g = \begin{cases} \frac{(k_o + k_c \exp(-(k_o + k_c)\Delta t))}{k_o + k_c} & \text{open} \\ \frac{(k_c + k_o \exp(-(k_o + k_c)\Delta t))}{k_o + k_c} & \text{closed} \end{cases} \quad [44]$$

where “open” and “closed” refer to the initial states. If p_g exceeds a uniform random number selected from the interval (0, 1), the gate remains unchanged. Otherwise the gate is switched. In the standard approach, the active site is simply turned off when the gate is closed. In the probability distribution approach, w_{ik} is set to one when the gate is closed and calculated according to Eq. [43] when it is open. Gated reaction simulations for simple cases have been reported elsewhere.⁷⁸ This method permits the inclusion of a gate into a calculation without actually simulating it. Another approach is to explicitly simulate the motion of the gate, as is discussed below in the simulation of flexible loops of TIM.

ACKNOWLEDGMENTS

This work was supported at the University of South Alabama in part by the donors of the Petroleum Research Fund, administered by the American Chemical Society, Cray Research, and IBM Corporation, and at the University of Houston by the Robert A. Welch Foundation, the National Institutes of Health (NIH), the National Center for Supercomputing Applications, and the San Diego Supercomputer Center. MKG is the recipient of the Howard Hughes Postdoctoral Fellowship for Physicians, and BAL is the recipient of an NIH predoctoral traineeship in the Houston Area Molecular Biophysics Training Program.

REFERENCES

1. C. L. Brooks III, M. Karplus, and B. M. Pettitt, *Adv. Chem. Phys.*, **71**, 1 (1988). Proteins: A Theoretical Perspective of Dynamics, Structure, and Thermodynamics.
2. J. A. McCammon and S. C. Harvey, *Dynamics of Proteins and Nucleic Acids*, Cambridge University Press, Cambridge, 1987.
3. M. E. Davis and J. A. McCammon, *Chem. Rev.*, **90**, 509 (1990). Electrostatics in Biomolecular Structure and Dynamics.
4. K. A. Sharp and B. Honig, *Annu. Rev. Biophys. Biophys. Chem.*, **19**, 301 (1990). Electrostatic Interactions in Macromolecules: Theory and Application.
5. S. C. Harvey, *Proteins: Struct., Funct., Genet.*, **5**, 78 (1989). Treatment of Electrostatic Effects in Macromolecular Modeling.
6. M. E. Davis, J. D. Madura, J. J. Sines, B. A. Luty, S. A. Allison, and J. A. McCammon, *Methods Enzymol.* **202**, 473 (1991). Diffusion-Controlled Enzymatic Reactions.
7. E. D. Getzoff, D. E. Cabelli, C. L. Fisher, H. E. Parge, M. S. Viezzoli, L. Banci, and R. A. Hallewell, *Nature*, **358**, 347 (1992). Faster Superoxide Dismutase Mutants Designed by Enhancing Electrostatic Guidance. J. A. McCammon, *Curr. Biol.* **2**, 585 (1992). Superperfect Enzymes.
8. D. B. Boyd, in *Reviews in Computational Chemistry*, Vol. 4, K. B. Lipkowitz and D. B. Boyd, Eds., VCH Publishers, New York, 1993, pp. 229–257. Compendium of Molecular Modeling Software. UHBD is available from Molecular Simulations Inc. DelPhi is available from BIOSYM. MEAD is described by D. Bashford and K. Gerwert, *J. Mol. Biol.*, **224**, 473 (1992). Electrostatic Calculations of the pK_a Values of Ionizable Groups in Bacteriorhodopsin. MEAD can be obtained by anonymous ftp from scripps.edu (192.42.82.27) or from the author, bashford@scripps.edu.
9. M. K. Gilson, K. A. Sharp, and B. H. Honig, *J. Comput. Chem.*, **9**, 327 (1987). Calculating the Electrostatic Potential of Molecules in Solution: Method and Error Assessment.
10. See e.g., D. Shortle, *Q. Rev. Biophys.* **25**, 205 (1992). Mutational Studies of Protein Structures and Their Stabilities.
11. See, e.g., R. Langen, G. D. Brayer, A. M. Berghuis, G. McLendon, F. Sherman, and A. Warshel, *J. Mol. Biol.*, **224**, 589 (1992). Effect of the Asn52-Ile Mutation on the Redox Potential of Yeast Cytochrome-*c*—Theory and Experiment.
12. V. M. Coghlan and L. E. Vickery, *J. Biol. Chem.*, **267**, 8932 (1992). Electrostatic Interactions Stabilizing Ferredoxin Electron Transfer Complexes—Disruption by Conservative Mutations.
13. J. H. Zhang, Z. P. Liu, T. A. Jones, L. M. Gierasch, and J. F. Sambrook, *Proteins: Struct., Funct., Genet.*, **13**, 87 (1992). Mutating the Charged Residues in the Binding Pocket of Cellular Retinoic Acid-Binding Protein Simultaneously Reduces Its Binding Affinity to Retinoic Acid and Increases Its Thermostability.
14. F. M. Richards, *Annu. Rev. Biophys. Bioeng.*, **6**, 151 (1977). Areas, Volumes, Packing and Protein Structure.

15. B. Lee and F. M. Richards, *J. Mol. Biol.*, **55**, 379 (1971). The Interpretation of Protein Structures: Estimation of Static Accessibility.
16. E. S. Reiner and C. J. Radke, *J. Chem. Soc. Faraday Trans.*, **86**, 3901 (1990). Variational Approach to the Electrostatic Free Energy in Charged Colloidal Suspensions: General Theory for Open Systems.
17. M. E. Davis and J. A. McCammon, *J. Comput. Chem.*, **12**, 909 (1991). Dielectric Boundary Smoothing in Finite Difference Solutions of the Poisson Equation: An Approach to Improve Accuracy and Convergence.
18. J. Warwicker and H. C. Watson, *J. Mol. Biol.*, **157**, 671 (1982). Calculation of Electric Potential in the Active Site Cleft Due to α -Helix Dipoles.
19. I. Klapper, R. Hagstrom, R. Fine, K. Sharp, and B. Honig, *Proteins: Struct., Funct., Genet.* **1**, 47 (1986). Focusing of Electric Fields in the Active Site of Cu-Zn Superoxide Dismutase: Effects of Ionic Strength and Amino-Acid Modification.
20. H. Nakamura and S. Nishida, *J. Phys. Soc. Japan*, **56**, 1609 (1987). Numerical Calculations of Electrostatic Potentials of Protein—Solvent Systems by the Self-Consistent Boundary Method.
21. M. E. Davis and J. A. McCammon, *J. Comput. Chem.*, **10**, 386 (1989). Solving the Finite Difference Linearized Poisson–Boltzmann Equation: A Comparison of Relaxation and Conjugate Gradient Methods.
22. A. Nicholls and B. Honig, *J. Comput. Chem.*, **12**, 435 (1991). A Rapid Finite-Difference Algorithm, Utilizing Successive Over-Relaxation to Solve the Poisson–Boltzmann Equation.
23. J. A. Meijerink and H. A. van der Vorst, *Math. Comput.*, **31**, 148 (1977). An Iterative Solution Method for Linear Systems of Which the Coefficient Matrix Is a Symmetric M -Matrix.
24. H. A. van der Vorst, *Comput. Phys. Commun.*, **53**, 223 (1989). ICCG and Related Methods for 3D Problems on Vector Computers.
25. M. Holst and F. Saied, *Multigrid Solution of the Poisson–Boltzmann Equation*, Technical Report UIUCDCS-R-92-1744, Department of Computer Science, University of Illinois at Urbana-Champaign, 1992.
26. K. A. Sharp and B. Honig, *J. Phys. Chem.*, **19**, 7684 (1990). Calculating Total Electrostatic Energies with the Nonlinear Poisson–Boltzmann Equation.
27. B. A. Luty, M. E. Davis, and J. A. McCammon, *J. Comput. Chem.*, **13**, 1114 (1992). Solving the Finite-Difference Non-Linear Poisson–Boltzmann Equation.
28. B. A. Luty, M. E. Davis, and J. A. McCammon, *J. Comput. Chem.*, **13**, 768 (1992). Electrostatic Energy Calculations by a Finite-Difference Method: Rapid Calculations of Charge–Solvent Interaction Energies.
29. M. K. Gilson and B. H. Honig, *Biopolymers*, **25**, 2097 (1986). The Dielectric Constant of a Folded Protein.
30. V. Mohan, M. E. Davis, J. A. McCammon, and B. M. Pettitt, *J. Phys. Chem.*, **96**, 6428 (1992). Continuum Model Calculations of Solvation Free Energies: Accurate Evaluation of Electrostatic Contribution.
31. S. Cabani, P. Gianni, V. Mollica, and L. Lepori, *J. Solution Chem.*, **10**, 563 (1981). Group Contributions to the Thermodynamic Properties of Non-Ionic Organic Solutes in Dilute Aqueous Solution.
32. J.-C. Arald, A. Nicholls, K. Sharp, B. Honig, A. Tempczyk, T. F. Hendrickson, and W. C. Still, *J. Am. Chem. Soc.*, **113**, 145 (1991). Electrostatic Contributions to Solvation Free Energy Perturbation and Continuum Calculations.
33. K. Linderstrom-Lang, *Compt. Rend. Trav. Lab. Carlsberg*, **15**, 1 (1924). The Ionization of Proteins. C. Tanford and J. G. Kirkwood, *J. Am. Chem. Soc.*, **79**, 5333 (1957). Theory of Protein Titration Curves. I. General Equations for Impenetrable Spheres.
34. W. H. Orttung, *Biochemistry*, **9**, 2394 (1970). Proton Binding and Dipole Moment of Hemoglobin. Refined Calculations. C. Tanford and R. Roxby, *Biochemistry*, **11**, 2192

- (1972). Interpretation of Protein Titration Curves. Application to Lysozyme. S. J. Shire, G. I. H. Hanania, and F. R. N. Gurd, *Biochemistry*, **13**, 2967 (1974). Electrostatic Effects in Myoglobin. Hydrogen Ion Equilibria in Sperm Whale Ferrimyoglobin.
35. W. E. Stites, A. G. Gittis, E. E. Lattman, and D. Shortle, *J. Mol. Biol.*, **221**, 7 (1991). In a Staphylococcal Nuclease Mutant the Side Chain of a Lysine Replacing Val-66 is Fully Buried in the Hydrophobic Core.
36. R. Varadarajan, D. G. Lambright, and S. G. Boxer, *Biochemistry*, **28**, 3771 (1989). Electrostatic Interactions in Wild-Type and Mutant Recombinant Human Myoglobins.
37. J. Sancho, L. Serrano, and A. R. Fersht, *Biochemistry*, **31**, 2253 (1992). Histidine Residues at the N- and C-Termini of α -Helices: Perturbed pK_a s and Protein Stability.
38. M. K. Gilson, A. A. Rashin, R. Fine, and B. Honig, *J. Mol. Biol.*, **183**, 503 (1985). On the Calculation of Electrostatic Interactions in Proteins.
39. D. Bashford and M. Karplus, *J. Phys. Chem.*, **95**, 9556 (1991). Multiple-Site Titration Curves of Proteins: An Analysis of Exact and Approximate Methods for Their Calculation.
40. P. Beroza, D. R. Fredkin, M. Y. Okamura, and G. Feher, *Proc. Natl. Acad. Sci. U.S.A.*, **88**, 5804 (1991). Protonation of Interacting Residues in a Protein by a Monte Carlo Method: Application to Lysozyme and the Photosynthetic Reaction Center of *Rhodobacter sphaeroides*.
41. A. S. Yang, M. R. Gunner, R. Sampogna, K. Sharp, and B. Honig, *Proteins: Struct., Funct., Genet.*, **15**, 252 (1993). On the Calculation of pK_a s in Proteins.
42. M. K. Gilson, *Proteins: Struct., Funct., Genet.*, **15**, 266 (1993). Multiple-Site Titration and Molecular Modelling: Two Rapid Methods for Computing Energies and Forces for Ionizable Groups in Proteins.
43. D. Bashford and M. Karplus, *Biochemistry*, **9**, 327 (1987). pK_a s of Ionizable Groups in Proteins: Atomic Detail from a Continuum Electrostatic Model.
44. K. Langsetmo, J. A. Fuchs, C. Woodward, and K. A. Sharp, *Biochemistry*, **30**, 7609 (1991). Linkage of Thioredoxin Stability to Titration of Ionizable Groups with Perturbed pK_a s.
45. D. Bashford and K. Gerwert, *J. Mol. Biol.*, **224**, 473 (1992). Electrostatic Calculations of the pK_a Values of Ionizable Groups in Bacteriorhodopsin.
46. S. Kurimatsu and K. Hamaguchi, *J. Biochem.*, **87**, 1215 (1980). Analysis of the Acid-Base Titration of Hen Lysozyme.
47. T. Imoto, *Biophys. J.*, **44**, 293 (1983). Electrostatic Free Energy of Lysozyme.
48. D. W. Urry, S. Q. Peng, and T. M. Parker, *Biopolymers*, **32**, 373 (1992). Hydrophobicity-Induced pK Shifts in Elastin Protein-Based Polymers.
49. J. A. Stratton, *Electromagnetic Theory*, McGraw-Hill, New York, 1941.
50. M. K. Gilson, M. E. Davis, B. A. Luty, and J. A. McCammon, *J. Phys. Chem.*, **97**, 3591 (1993). Computation of Electrostatic Forces on Solvated Molecules Using the Poisson-Boltzmann Equation.
51. D. Henderson, L. Blum, and J. L. Lebowitz, *J. Electroanal. Chem.*, **102**, 315 (1979). An Exact Formula for the Contact Value of the Density Profile of a System of Charged Hard Spheres Near a Charged Wall.
52. C. Niedermeier and K. Schulten, *Mol. Simulation*, **8**, 361 (1992). Molecular Dynamics Simulations in Heterogeneous Dielectric and Debye-Hückel Media—Application to the Protein Bovine Pancreatic Trypsin Inhibitor.
53. K. Sharp, *J. Comput. Chem.*, **12**, 454 (1991). Incorporating Solvent and Ion Screening into Molecular Dynamics Using the Finite-Difference Poisson-Boltzmann Method.
54. R. J. Zauhar, *J. Comput. Chem.*, **12**, 575 (1991). The Incorporation of Hydration Forces Determined by Continuum Electrostatics into Molecular Mechanics Simulations.
55. D. Banner, A. Bloomer, G. Petsko, D. Phillips, and I. Wilson, *Biochem. Biophys. Res. Commun.*, **72**, 146 (1976). Atomic Coordinates for Triose Phosphate Isomerase from Chicken Muscle.

56. W. L. Jorgensen and J. Tirado-Rives, *J. Am. Chem. Soc.*, **110**, 1657 (1988). The OPLS Potential Function for Proteins. Energy Minimizations for Crystals of Cyclic Peptides and Crambin.
57. L. Jarvis, C. Huang, T. Ferrin, and R. Langridge, *UCSF MIDAS User's Manual*, San Francisco, CA, 1986.
58. W. F. van Gunsteren and H. J. C. Berendsen, *Mol. Phys.*, **45**, 637 (1982). Algorithms for Brownian Dynamics.
59. D. L. Ermak and J. A. McCammon, *J. Chem. Phys.*, **69**, 1352 (1978). Brownian Dynamics with Hydrodynamic Interactions.
60. S. A. Allison and J. A. McCammon, *J. Phys. Chem.*, **89**, 1072 (1985). Dynamics of Substrate Binding to Copper Zinc Superoxide Dismutase.
61. S. A. Allison, G. Ganti, and J. A. McCammon, *Biopolymers*, **24**, 1323 (1985). Simulation of the Diffusion-Controlled Reaction Between Superoxide and Superoxide Dismutase. I. Simple Models.
62. A. Iniesta and J. G. de la Torre, *J. Chem. Phys.*, **92**, 2015 (1990). A Second-Order Algorithm for the Simulation of the Brownian Dynamics of Macromolecular Models.
63. S. A. Allison, S. H. Northrup, and J. A. McCammon, *J. Chem. Phys.*, **83**, 2894 (1985). Extended Brownian Dynamics of Diffusion-Controlled Reactions.
64. K. Sharp, R. Fine, and B. Honig, *Science*, **236**, 1460 (1987). Computer Simulations of the Diffusion of a Substrate to an Active Site of an Enzyme.
65. T. Head-Gordon and C. L. Brooks, III, *J. Phys. Chem.*, **91**, 3342 (1987). The Role of Electrostatics in the Binding of Small Ligands to Enzymes.
66. S. A. Allison, R. J. Bacquet, and J. A. McCammon, *Biopolymers*, **27**, 251 (1988). Simulation of the Diffusion-Controlled Reaction Between Superoxide and Superoxide Dismutase. II. Detailed Models.
67. S. H. Northrup, J. O. Boles, and J. C. L. Reynolds, *Science*, **241**, 67 (1988). Brownian Dynamics of Cytochrome *c* and Cytochrome *c* Peroxidase Association.
68. J. D. Madura and J. A. McCammon, *J. Phys. Chem.*, **93**, 7285 (1989). Brownian Dynamics Simulation of Diffusional Encounters Between Triose Phosphate Isomerase and D-Glyceraldehyde Phosphate.
69. G. Ganti, J. A. McCammon, and S. A. Allison, *J. Phys. Chem.*, **89**, 3899 (1985). Brownian Dynamics of Diffusion-Controlled Reactions: The Lattice Method.
70. J. J. Sines, S. A. Allison, and J. A. McCammon, *J. Comput. Chem.*, **13**, 66 (1992). Kinetic Effects of Multiple Charge Modifications in Enzyme-Substrate Reactions.
71. R. C. Tan, T. N. Truong, J. A. McCammon, and J. L. Sussman, *Biochemistry*, **32**, 401 (1993). Acetylcholinesterase: Electrostatic Steering Increases the Rate of Ligand Binding.
72. S. H. Northrup, S. A. Allison, and J. A. McCammon, *J. Chem. Phys.*, **80**, 1517 (1984). Brownian Dynamics Simulation of Diffusion-Influenced Bimolecular Reactions.
73. G. Wilemski and M. Fixman, *J. Chem. Phys.*, **58**, 4009 (1973). General Theory of Diffusion-Controlled Reactions.
74. H.-X. Zhou, *J. Chem. Phys.*, **92**, 3092 (1990). On the Calculation of Diffusive Reaction Rates Using Brownian Dynamics Simulations.
75. B. A. Luty, H. X. Zhou, and J. A. McCammon, *J. Chem. Phys.*, **97**, 5682 (1992). Calculation of Diffusive Reaction Rates Using Brownian Dynamics Simulations.
76. G. Lamm and K. Schulten, *J. Chem. Phys.*, **78**, 2713 (1983). Extended Brownian Dynamics. II. Reactive, Nonlinear Diffusion.
77. S. H. Northrup, M. S. Curvin, S. A. Allison, and J. A. McCammon, *J. Chem. Phys.*, **84**, 2196 (1986). Optimization of Brownian Dynamics Methods for Diffusion-Influenced Rate Constant Calculations.

78. S. A. Allison, J. A. McCammon, and J. J. Sines, *J. Phys. Chem.*, **94**, 7133 (1990). Brownian Dynamics Simulations of Diffusion-Influenced Reactions. Inclusion of Intrinsic Reactivity and Gating.
79. J. C. Reynolds, K. F. Cooke, and S. H. Northrup, *J. Phys. Chem.*, **94**, 985 (1990). Electrostatics and Diffusional Dynamics in the Carbonic Anhydrase Active Site Channel.
80. S. H. Northrup, J. O. Boles, and J. C. Reynolds, *J. Phys. Chem.*, **91**, 5991 (1987). Electrostatic Effects in the Brownian Dynamics of Association and Orientation of Heme Proteins.
81. M. E. Davis, J. D. Madura, B. A. Luty, and J. A. McCammon, *Comput. Phys. Commun.*, **62**, 187 (1991). Electrostatics and Diffusion of Molecules in Solution: Simulations with the University of Houston Brownian Dynamics Program.
82. M. V. Smoluchowski, *Phys. Z.*, **17**, 557 (1916). Three Lectures on Diffusion, Brownian Movement, and Coagulation of Colloidal Particles.
83. W. Alber and J. Knowles, *Biochemistry*, **25**, 5627 (1976). Free-Energy Profile for the Reaction Catalysed by Triose Phosphate Isomerase.
84. S. Blacklow, R. Raines, W. Lim, P. Zamore, and J. Knowles, *Biochemistry*, **27**, 1158 (1988). Triose Phosphate Isomerase Catalysis Is Diffusion Controlled.
85. J. Knowles, *Nature*, **350**, 121 (1991). Enzyme Catalysis: Not Different, Just Better.
86. B. A. Luty, R. C. Wade, J. D. Madura, M. E. Davis, J. M. Briggs, and J. A. McCammon, *J. Phys. Chem.*, **97**, 233 (1993). Brownian Dynamics Simulations of Diffusional Encounters Between Triose Phosphate Isomerase and Glyceraldehyde Phosphate: Electrostatic Steering of Glyceraldehyde Phosphate.
87. D. Banner, A. Bloomer, G. Petsko, D. Phillips, C. Pogson, I. Wilson, P. Corran, A. Furth, J. Milman, R. Offord, J. Priddle, and S. Waley, *Nature*, **255**, 609 (1975). Structure of Chicken Muscle Triose Phosphate Isomerase Determined Crystallographically at 2.5 Å Resolution Using Amino Acid Sequence Data.
88. T. Alber, D. Banner, A. Bloomer, G. Petsko, D. Phillips, P. Rivers, and I. Wilson, *Phil. Trans. R. Soc. Lond.*, **293**, 159 (1981). On the Three-Dimensional Structure and Catalytic Mechanism of Triose Phosphate Isomerase.
89. F. C. Bernstein, T. F. Koetzle, G. J. B. Williams, E. F. Meyer, Jr., M. D. Brice, J. R. Rodgers, O. Kennard, T. Shimanouchi, and M. Tasumi, *J. Mol. Biol.*, **112**, 535 (1977). The Protein Data Bank: A Computer-Based Archival File for Macromolecular Structures.
90. N. S. Sampson and J. R. Knowles, *Biochemistry*, **31**, 8482 (1992). Segmental Movement: Definition of the Structural Requirements for Loop Closure in Catalysis by Triose Phosphate Isomerase.
91. N. S. Sampson and J. R. Knowles, *Biochemistry*, **31**, 8488 (1992). Segmental Motion in Catalysis: Investigation of a Hydrogen Bond Critical for Loop Closure in the Reaction of Triose Phosphate Isomerase.
92. T. Alber, W. A. Gilbert, D. R. Ponzi, and G. A. Petsko, in *Ciba Found. Symp. 93, Mobility and Function in Proteins and Nucleic Acids*, Pitman, London, 1983, pp. 4–24. The Role of Mobility in the Substrate Binding and Catalytic Machinery of Enzymes.
93. D. Pompliano, A. Peyman, and J. Knowles, *Biochemistry*, **29**, 3186 (1990). Stabilization of a Reaction Intermediate as a Catalytic Device: Definition of the Functional Role of the Flexible Loop in Triose Phosphate Isomerase.
94. R. Wade, B. Luty, M. Davis, J. Madura, and J. McCammon, *Biophys. J.*, **64**, 9 (1992). Gating of the Active Site of Triose Phosphate Isomerase: Brownian Dynamics Simulations of Flexible Peptide Loops in the Enzyme.
95. M. Levitt and A. Warshel, *Nature*, **253**, 694 (1975). Computer Simulation of Protein Folding.
96. M. Levitt, *J. Mol. Biol.*, **104**, 59 (1976). A Simplified Representation of Protein Conformations for Rapid Simulation of Protein Folding.
97. J. McCammon, S. Northrup, M. Karplus, and R. Levy, *Biopolymers*, **19**, 2033 (1980). Helix–Coil Transitions in a Simple Polypeptide Model.

-
98. J. P. Ryckaert, G. Ciccotti, and H. J. C. Berendsen, *J. Comput. Phys.*, **23**, 327 (1977). Numerical Integration of the Cartesian Equations of Motion of a System with Constraints: Molecular Dynamics of *n*-Alkanes.
 99. E. Lolis and G. Petsko, *Biochemistry*, **29**, 6619 (1990). Crystallographic Analysis of the Complex Between Triose Phosphate Isomerase and 2-Phosphoglycolate at 2.5 Å Resolution: Implications for Catalysis.
 100. R. Wierenga, M. Noble, J. Postma, H. Groendijk, K. Kalk, W. Hol, and F. Opperdoes, *Proteins: Struct., Funct., Genet.*, **10**, 33 (1991). The Crystal Structure of the Open and the Closed Conformation of the Flexible Loop of Trypanosomal Triose Phosphate Isomerase.
 101. D. Joseph, G. Petsko, and M. Karplus, *Science*, **249**, 1425 (1990). Anatomy of a Conformational Change: Hinged "Lid" Motion of the Triose Phosphate Isomerase Loop.
 102. A. Szabo, D. Shoup, S. Northrup, and J. McCammon, *J. Chem. Phys.*, **77**, 4484 (1982). Stochastically Gated Diffusion-Influenced Reactions.